Volume 302, number 1, 89–96 FEBS 10971 May 1992
© 1992 Federation of European Biochemical Societies 00145793/92/$5.00

Solution structure of FK506 bound to FKBP-12

Christopher A. Lepre, John A. Thomson and Jonathan M. Moore

Vertex Pharmaceuticals Incorporated, 40 Allston Street, Cambridge, MA 02139-4211, USA

Received 6 March 1992; revised version received 10 March 1992

The complex of the immunosuppressant FK506 bound to FKBP-12 has been studied in solution using ^{1}H and inverse-detected ^{13}C NMR methods. The resonances of bound, ^{13}C-labelled FK506 were assigned and a set of 66 intraligand NOE distance restraints were used to calculate the structure of the bound ligand by distance geometry and restrained molecular dynamics methods. The structure of bound FK506 in solution closely resembles that seen in the X-ray structure [17], except for the allyl region. The differences reflect the influence of intermolecular crystal contacts and have implications for interpretation of the interaction of the FK506/FKBP complex with its putative biological receptor.

FK506; FKBP; Peptidyl-prolyl *cis-trans* isomerase; NMR; Immunophilin

1. INTRODUCTION

FK506 and cyclosporin (CsA) are potent immunosuppressants that have been shown to inhibit signal transduction pathways leading to T-cell activation [1]. These drugs appear to act in the early stages of T-cell activation by blocking pathways leading to transcription of IL-2 genes [2–5]. The major binding proteins for these drugs, termed immunophilins, are the FK506 binding protein (FKBP-12) and cyclophilin (CyP), respectively. Recently it has been shown that a calcium and calmodulin dependent protein phosphatase, calcineurin, binds and is inhibited by the binary complexes of FK506 with FKBP-12 and cyclosporin with cyclophilin [6].

To better understand the molecular mechanism of inhibition of immunophilin/drug interactions, several groups have directed efforts towards determination of the three-dimensional structures of immunophilins and immunophilin/drug complexes [7–16]. In this paper, we report the structure of ^{13}C-labelled FK506 in the monomeric complex with human recombinant FKBP-12 (hrFKBP-12). Heteronuclear and isotope filtered experiments have been used to selectively observe and assign ^{1}H signals arising from ^{13}C-enriched FK506 bound to unlabelled hrFKBP-12. Solution structures for bound FK506 have been generated by distance geometry methods following quantitation of NOEs from ^{13}C-attached protons, and the structures refined by restrained molecular dynamics.

Abbreviations: COSY, correlated spectroscopy; CsA, cyclosporin A; CyP, cyclophilin; DG, distance geometry; DQ, double quantum; DQF, double quantum filtered; FKBP-12, FK506 binding protein (11.8 kDa); GARP, globally optimized alternating-phase rectangular pulses; hrFKBP-12, human recombinant FKBP-12; HMQC, heteronuclear multiple quantum coherence spectroscopy; HSQC, heteronuclear single quantum coherence spectroscopy; HSQC-NOESY, heteronuclear single quantum coherence-nuclear Overhauser enhancement spectroscopy; MD, molecular dynamics; NMR, nuclear magnetic resonance; NOE, nuclear Overhauser enhancement; NOESY, two-dimensional NOE spectroscopy; TOCSY, total correlation spectroscopy; 2D, two dimensional.

Correspondence address: J.M. Moore, Vertex Pharmaceuticals Incorporated, 40 Allston St., Cambridge, MA 02139-4211, USA. Fax: (1) (617) 576-2109.

2. MATERIALS AND METHODS

Isotopically labelled FK506 was produced by growing *Streptomyces* [17,18] in a fermentation medium containing uniformly labelled [^{13}C]-glucose. The carbons of the pipecolic acid were not enriched because this moiety is biosynthetically derived entirely from amino acids. All other carbon sites contained 51% to 98% ^{13}C. hrFKBP-12 was expressed (S. Chambers, unpublished) and purified as described previously [7]. The final NMR sample contained 5.3 mM FK506/FKBP-12 complex in 50 mM potassium phosphate buffer (90% H_2O, 10% D_2O) at pH 7.0.

All NMR spectra were collected at 303 K on a Bruker AMX-500 spectrometer equipped with an X32 computer. Data were processed with Bruker UXNMR software, and peak integration was carried out using the EASY (ETH Automated Spectroscopy) program [9]. HSQC, HMQC-TOCSY (τ_m = 32 ms), and HSQC-NOESY (τ_m = 80 ms) spectra were collected in accordance with methods described in [20,21]. $^{13}C(\omega_1)$-$^{13}C(\omega_2)$-double-half-filtered NOESY spectra (τ_m = 80 ms) were collected as described in [22,23]. Subspectra were combined on the X32 computer using in-house software. ^{13}C COSY, ^{1}H 2QF-COSY [24], NOESY (τ_m = 80 ms) [25], sensitivity-enhanced TOCSY (τ_m = 70 ms) [26], and double quantum (τ_m = 32 ms) [27,28] experiments were acquired using standard pulse sequences and phase cycling.

The structure of FK506 was calculated from a set of 66 NOEs integrated in the HSQC-NOESY spectrum (τ_m = 80 ms). NOE intensities were scaled to account for the level of ^{13}C enrichment and the number of attached protons. Some spin-diffusion effects were observed, particularly between protons within ring systems. Accordingly, a conservative calibration of distance restraints was employed using NOEs between neighboring methylenes. Upper bound corrections were added to restraints involving pseudoatoms. Lower bounds of 1.80 Å were used in all cases. Based on the analysis of vicinal ^{1}H–^{1}H

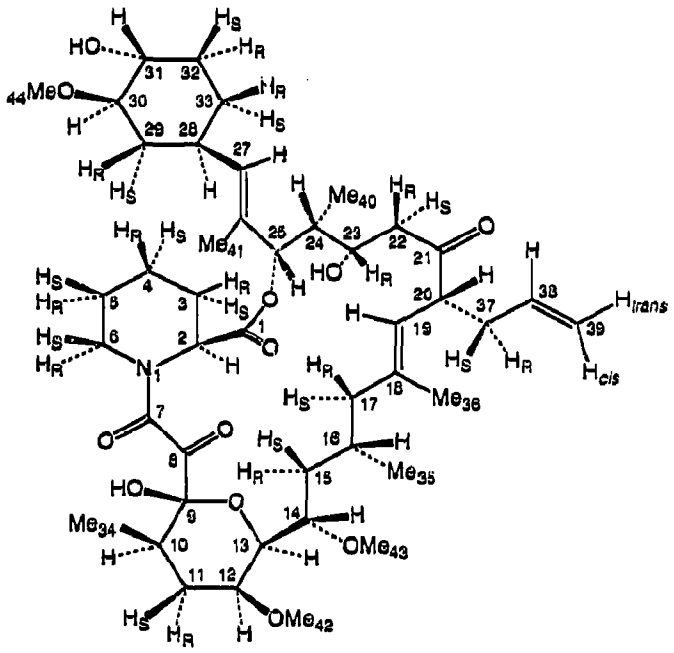

Fig. 1. Primary structure of FK506. Cambridge Data Base numbering is used. This numbering differs slightly from a previously published scheme [35,36].

couplings within the pipecolinyl ring, dihedral angles were restrained to within ±60° of values consistent with the chair conformation.

Using these distance restraints, 200 initial structures were generated by using the DGII distance geometry algorithm [29] with tetrangle smoothing [30] within InsightII (Biosym Technologies). The 50 DGII structures having the lowest error functions [29] were then subjected to restrained molecular dynamics refinement using Discover (Biosym Technologies). The system was heated to 1500 K over 1 ps, while increasing the force constant for the NMR restraints to 36 kcal·mol^{-1}·Å^{-2}. After equilibrating for 8 ps at 1500 K, the system was cooled exponentially to 300 K over 7 ps, followed by minimization in the presence of the NMR restraints.

Although the final MD-refined structures had approximately equal restraint energies (all within 0.1 kcal), these structures fell into two distinct families based upon total energy. The set of 43 lower energy structures contained 39 with a *trans* amide conformation, while the second family, with 2–3 kcal higher total energy, consisted of seven structures, of which five possessed a *cis* amide geometry. Of the lower energy structures, the 39 with *trans* amide conformation were selected for rmsd analysis.

3. RESULTS AND DISCUSSION

3.1. *Assignment of bound FK506*

The stepwise scalar connectivities observed in the ^{13}C COSY spectrum (Fig. 2) formed the basis for assignment of the ^{13}C and ^{1}H resonances of bound FK506, HSQC, HMQC-TOCSY, and HSQC-NOESY spectra were used to obtain the chemical shifts of the attached protons. The three methoxy resonances were distinguished by their intensities and lack of nearest-neighbor couplings and were assigned on the basis of NOEs to the protons attached to the adjoining carbon.

The ^{13}C resonances of the pipecolic acid moiety (C1 to C6) could not be assigned because the carbons were not isotopically enriched. The pipecolinyl proton resonances, however, shift upfield dramatically upon binding to FKBP-12 and are well resolved. Unambiguous patterns of scalar couplings and NOEs provided diastereotopic proton assignments for all pipecolinyl protons and indicated that the ring adopts a chair conformation, in agreement with an earlier study [31]. All chemical shift assignments are listed in Table I.

In this work, HSQC-NOESY provided many more unambiguous intraligand NOEs and better sensitivity than the double-half-filtered NOESY spectrum. Intraligand NOEs were located in the HSQC-NOESY spectrum by their characteristic square pattern of crosspeaks (Fig. 3). When the origins of NOEs were in doubt, only those possessing a symmetry-related partner were used. Stereospecific assignments of methylene protons were made by comparing NOE intensities between methylene and neighboring protons, using a set of initial structures (calculated using pseudoatoms) to provide relative distances.

3.2. *Conformation of bound FK506*

The network of NOE distance restraints used in the structure calculations is shown in Fig. 4. A number of long-range NOE restraints were essential for defining the global conformation of the macrocycle. The position of the pyranose ring (C9-C13) was dictated by NOEs from 42-OMe to 41-Me, and from 13-CH to 24-CH and 41-Me. NOEs from the pipecolinyl methylene protons (C4-*pro R*, C5-*pro S*, C6-*pro R* and *pro S*) to 40-Me define its orientation. The local conformation of the macrocycle backbone from C14 to C26 was defined by a series of medium range NOEs. The relative position of the cyclohexane ring (C28–C33) is well defined by NOEs to the macrocycle, namely, 41-Me to 28-CH and 30-CH, as well as a four-spin network of NOEs from 28-CH and 33-CH$_2$ to 27-CH, and from 27-CH to 23-CH.

There are no protons in the region from N1 to C8, so local restraints are not available to define the conformation about the amide linkage (N1–C7). The amide geometry is instead defined globally by NOEs from the pipecolinyl and pyranose rings to 40-Me. In the final NMR structures, 39 of the 43 lowest energy structures exhibited the trans conformation, leading us to conclude that this is the most likely conformation in solution.

The initial 50 DGII and final 39 MD-refined NMR structures of FK506 are shown in Fig. 5, top and middle. None of the final structures contained more than two violations of the NOE restraints, nor any greater than 0.1 Å. The conformation of the bound ligand is very well defined; the average rmsd from the average structure is 0.28 Å for heavy atoms and 0.62 Å for all atoms. The narrow conformational envelope occupied

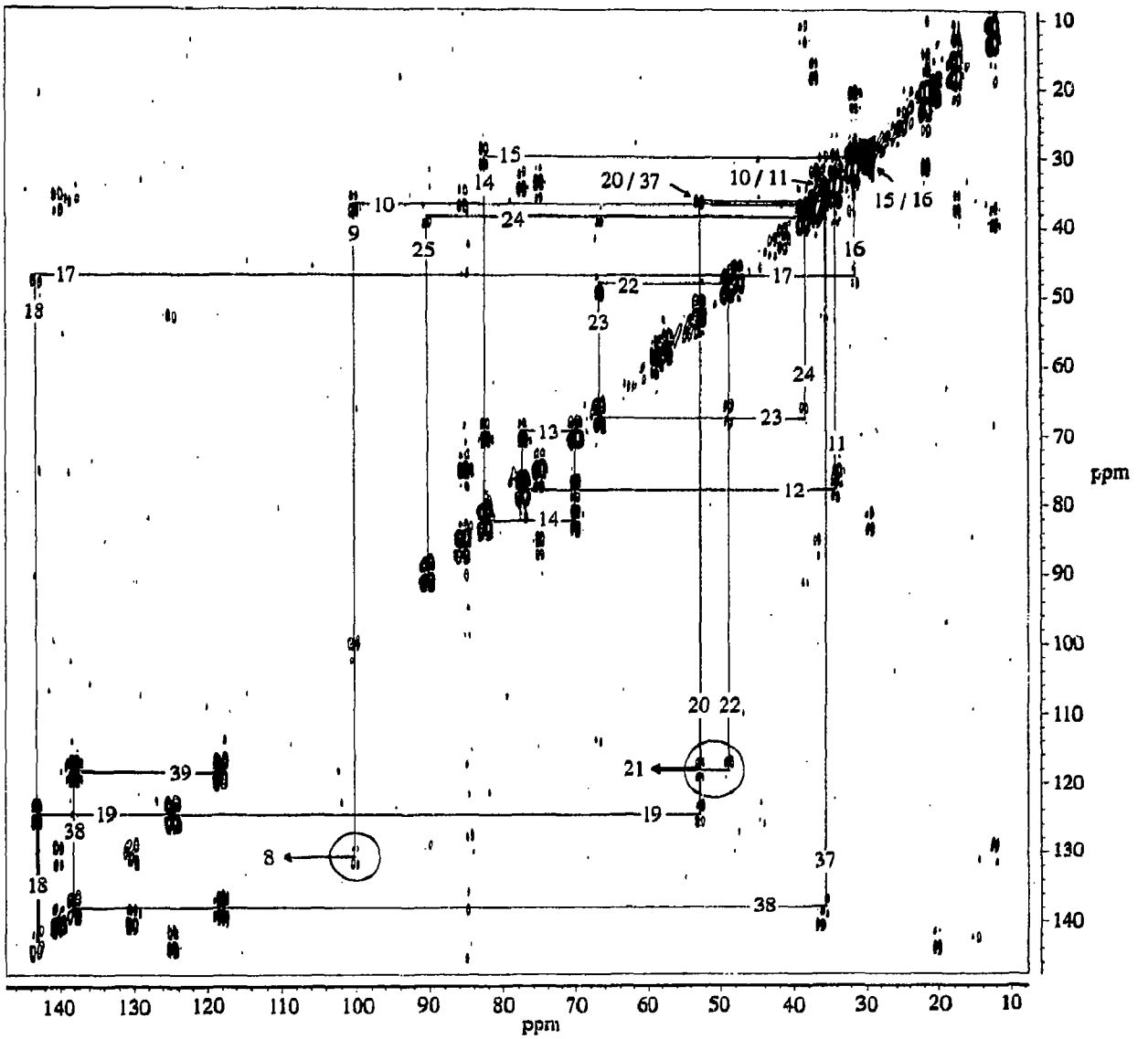

Fig. 2. [^{1}H] ^{13}C COSY spectrum at 125.76 MHz of ^{13}C-labelled FK506 bound to hrFKBP-12. Stepwise connectivities are illustrated for the macrocycle backbone carbons (C10 to C26) as well as the allylic group (C35 to C37). The carbonyl region (not shown) is folded in the F1 dimension; circled crosspeaks arise from C9 and C22, which have folded into the displayed region. Experimental parameters are: spectral width, 33,333 Hz in $\omega 2$, 20,123 Hz in $\omega 1$; 704 scans for each of 128 t_1 increments; WALTZ-16 hetero-decoupling [37] during t_2.

by the final structures is partly a consequence of the relatively high number of NMR restraints and the inherently limited flexibility of the macrocycle ring. In addition, there is a tendency for energy minimization to produce structures that share a common, lowest energy conformation.

Comparison of the average NMR structure with the x-ray structure [11] (Fig. 5, bottom) reveals overall similarity. The only significant differences occur in the region of the allyl group (C37 to C39). This group adopts multiple conformations in the family of refined structures, owing to its rapid motion and the consequent absence of NOE restraints. Direct exponential evidence for the motional flexibility of this group is provided by the narrow linewidths of its NMR resonances, and the unusually weak intensity of the 38-CH to 39-CH_2 NOEs.

A slight difference is found in the position of the cyclohexyl ring relative to its orientation in the crystal structure. Prior to MD refinement, the DG structures exhibit a range of conformations for the cyclohexyl ring that encompasses the position found in the x-ray structure (Fig. 5). MD simulations run in the presence of time-averaged restraints [32,33] indicate that the NOE restraints are insufficient to precisely define the orientation of this ring, instead allowing it to pivot through a range of angles. Hence, the precise orientation of this ring in the final MD-refined NMR structures is apparently dictated partly by the MD force field. The application of time-averaged restraints to this system (D.

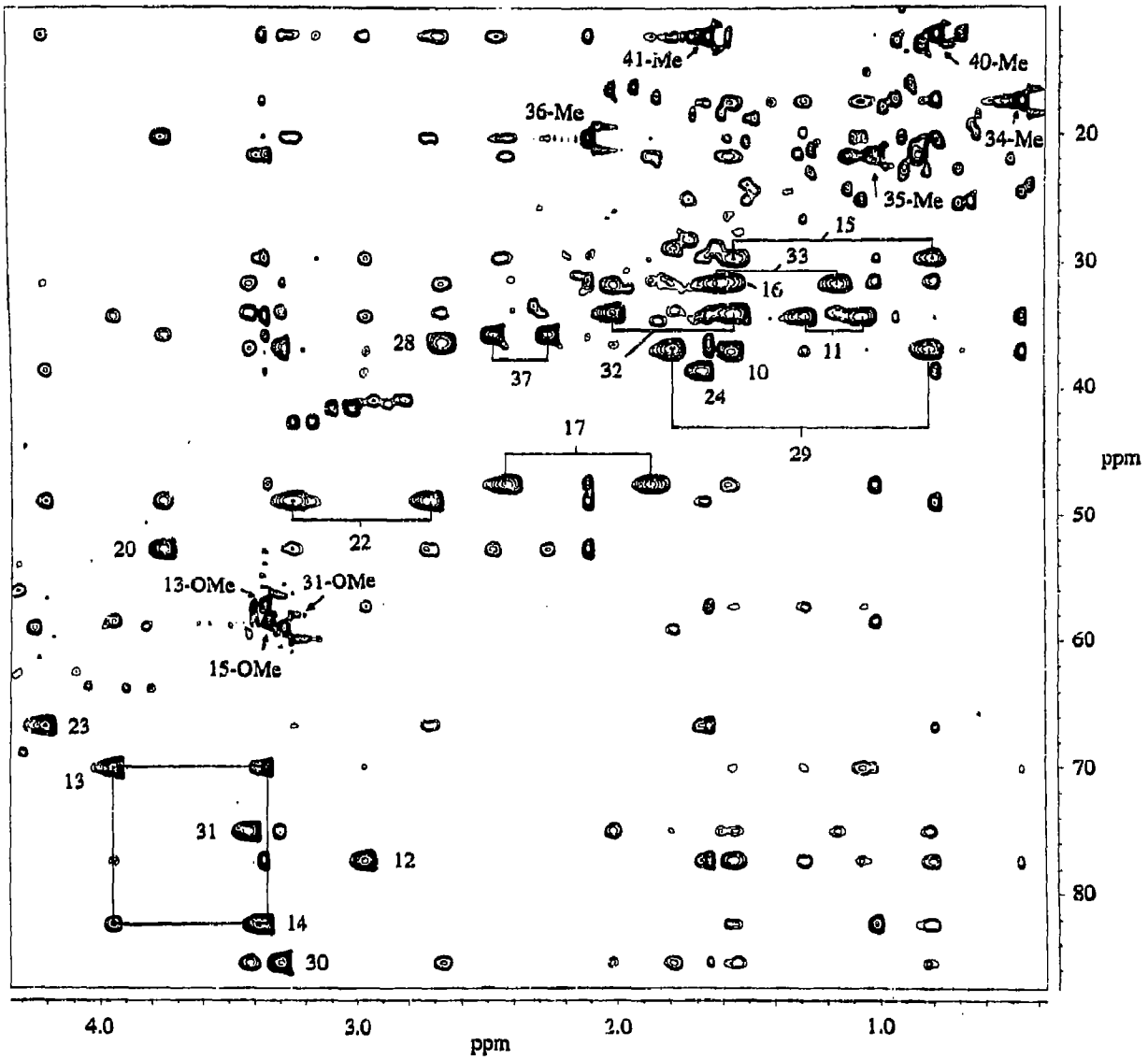

Fig. 3. HSQC-NOESY spectrum (τ_m = 80 ms) of ^{13}C-labelled FK506 bound to hrFKBP-12, showing the upfield region. HSQC peaks are labelled according to carbon number. Pairs of methylene HSQC peaks are connected by brackets. The box illustrates a typical set of symmetry-related intraligand NOEs. Spurious crosspeaks arising from intense protein and pipecolinyl signals were identified on the basis of their distinctive appearance in the related HSQC and HMQC-TOCSY spectra. Experimental parameters are: spectral width, 5,000 Hz in ω2, 27,672 Hz in ω1; 64 scans for each of 400 t_1 increments; GARP-2 hetero-decoupling [38] during t_2.

Pearlman, unpublished) will be discussed in detail elsewhere.

3.3. *Contacts between FK506 and hrFKBP-12*

A number of close contacts between FK506 and the side chains in the binding cleft of hr-FKBP-12 were evident in the HSQC-NOESY and ^{13}C (ω1, ω2) double-half-filtered NOESY experiments. The ligand protons involved in these contacts are indicated in Fig. 4. Several FKBP-12 side-chain spin systems were identified from 2D ^{1}H spectra, and tentative assignments were made by comparison with the published X-ray structure [11].

The large upfield shifts of the 3-CH_2 and 4-CH_2 protons observed upon binding to hr-FKBP-12 provide evidence for their proximity to aromatic systems. Protons located along the outside edge of pipecolinyl ring (3-, 4-, and 5-CH_2) exhibit NOEs to aromatic side chains located deep within the binding pocket. One of these nearby side chains gives rise to a distinctive set of four coupled resonances in COSY and DQ spectra (not shown), thus identifying it as Trp-59, in agreement with an earlier study [31]. Other NOEs between the pipecolinyl group and aromatic protein resonances suggest interactions with ring protons of Tyr-82 and Tyr-26.

One of the above-mentioned tyrosine ring spin systems exhibits many NOEs to the ligand, including 10-CH, 34-Me, and 11-CH_2 on the pyranose ring, and

Table I

^1H and ^{13}C chemical shifts for FK506 bound to hrFKBP-12 at pH 7.0 and 303 K[a]

Carbon chemical shifts (ppm)	Proton chemical shifts (ppm)	
Site	^{13}C shift	^1H shifts
1-CO	NA[b]	
2-CH	NA	4.49 (eq)[d]
3-CH_2	NA	−1.13 pro-S[c] (ax) 0.22 pro-R (eq)
4-CH_2	NA	−1.91 pro-S (eq) −0.43 pro-R (ax)
5-CH_2	NA	−1.06 pro-R (ax) −0.75 pro-S (eq)
6-CH_2	NA	3.14 pro-R (eq) −2.45 pro-S (ax)
7-CO	169.8	
8-CO	199.3	
9-C[e]	100.1	
10-CH	36.4	1.56
11-CH_2	34.2	1.28 pro-R 1.06 pro-S
12-CH	77.3	2.97
13-CH	70.0	3.95
14-CH	82.3	3.35
15-CH_2	29.5	1.55 pro-R 0.80 pro-S
16-CH	31.3	1.58
17-CH_2	47.4	1.84 pro-S 2.43 pro-R
18-C	143.1	
19-CH	124.7	4.81
20-CH	52.6	3.76
21-CO	212.2	
22-CH_2	48.8	2.74[f] 3.26[f]
23-CH	66.7	4.21
24-CH	38.5	1.69
25-CH	90.0	5.32
26-C	130.1	

Table I cont.

Carbon chemical shifts (ppm)	Proton chemical shifts (ppm)	
Site	^{13}C shift	^1H shifts
27-CH	140.2	5.36
28-CH	36.2	2.67
29-CH_2	36.2	0.82 pro-R 1.78 pro-S
30-CH	85.4	3.30
31-CH	75.1	3.42
32-CH_2	34.0	2.02 pro-S 1.55 pro-R
33-CH_2	31.5	1.15 pro-R 1.61 pro-S
34-Me	17.3	0.46
35-Me	21.4	1.02
36-Me	20.1	2.11
37-CH_2	35.6	2.27[f] 2.48[f]
38-CH	138.0	5.81
39-CH_2	118.2	5.06 *trans* 5.12 *cis*
40-Me	12.1	0.79
41-Me	12.1	1.70
42-OMe	57.3	3.36
43-OMe	58.5	3.35
44-OMe	85.4	3.30

[a] ^1H chemical shifts are referenced to H_2O at 4.73 ppm and ^{13}C shifts to external [^{13}C]acetate in phosphate buffer.
[b] Not assigned, because the pipecolinyl carbons were not isotopically enriched.
[c] pro-S and pro-S denote the stereo-specific assignments of prochiral centers.
[d] (ax) and (eq) denote axial and equatorial positions.
[e] quaternary carbon.
[f] protons not stereo-specifically assigned.

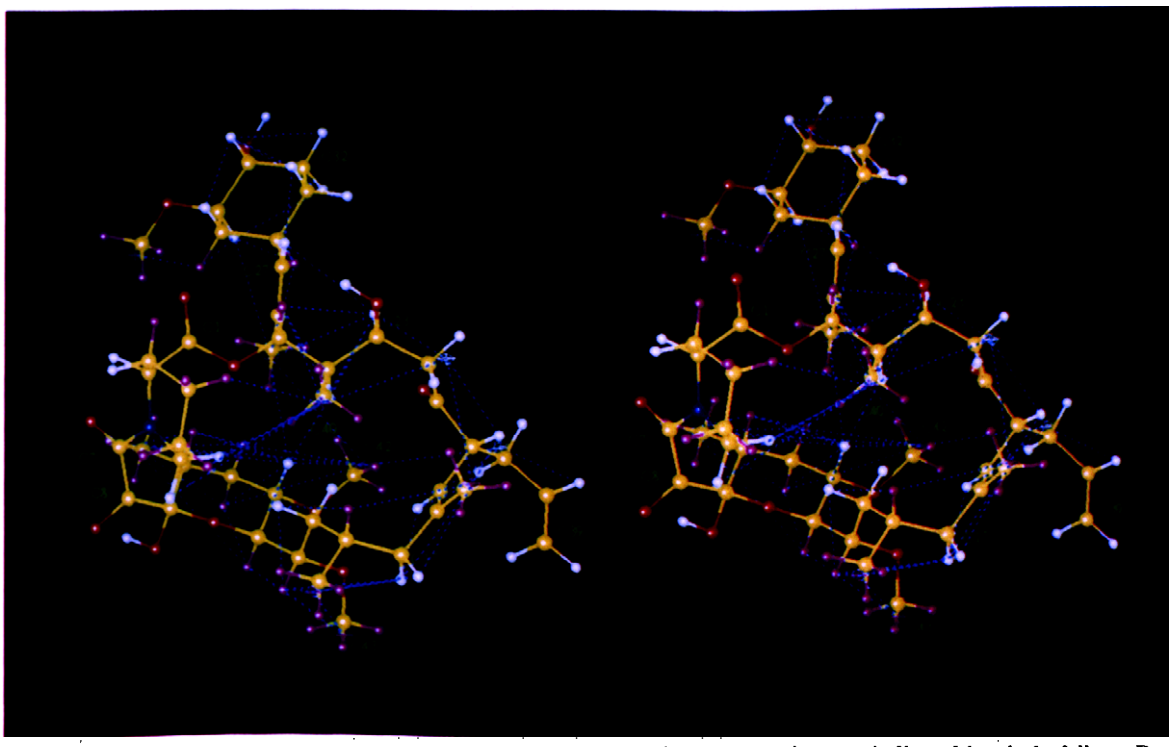

Fig. 4. Ball and stick stereo representation of the average NMR structure. Distance restraints are indicated by dashed lines. Pseudoatoms are depicted by small octahedrons. Ligand protons that exhibit NOE contacts with protein side chains are colored purple.

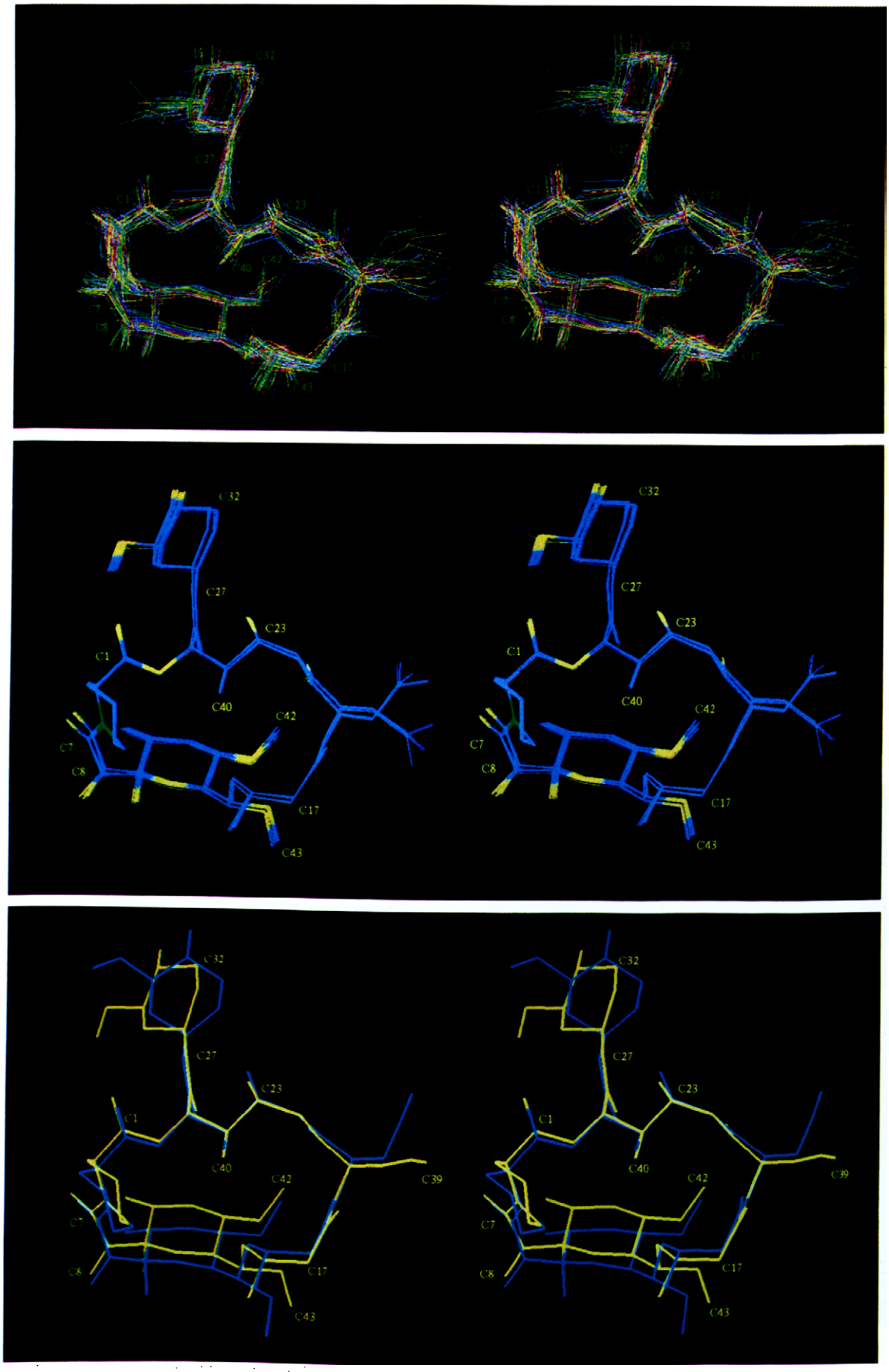
C32
C27
C23
C1
C40
C42
C7
C8
C17
C43
C39

Fig. 5. (top) Stereoview of the 50 DGII structures with the lowest total error functions. Only heavy atoms are shown. (middle) Stereoview of the 39 MD-refined NMR structures with the lowest total energies and *trans* amide configurations. Heavy atoms are coded: carbon (blue), oxygen (yellow), nitrogen (green). (bottom) Stereoview of the average NMR structure (yellow) superimposed upon the *X-ray* structure (cyan) of reference [11]. Only heavy atoms are shown.

←

41-Me, 28-CH, 29-CH2, and 31-OMe on one edge of the cyclohexyl moiety. Examination of the crystal structure indicates that this tyrosine residue is most likely Tyr-82.

Another aromatic spin system, identified as a phenylalanine on the basis of scalar couplings, gives rise to NOEs to 16-CH, 35-Me, 36-Me, and 41-Me. On the basis of the crystal structure, this residue is most likely Phe-46. These close contacts provide further evidence that the region of FK506 from C3 to C16 is involved in protein binding. On the other hand, no NOEs are observed between the protein and the well-resolved resonances of the macrocycle in the region from 20-CH to 23-CH, or from the allylic group, suggesting that this part of the molecule is exposed to solvent. The overall pattern of ligand/protein contacts agrees with that seen in previous X-ray crystallographic [11,12,16] and NMR studies [15,34] of FKBP-12/ligand complexes.

4. CONCLUSIONS

In solution, FK506 binds to hrFKBP-12 in a single conformation closely resembling that seen in the X-ray structures. The principal exception is the allyl region, which is more disordered in solution. In the X-ray structures, this moiety packs against the allyl group from a second, symmetry-related complex molecule in the unit cell [16], indicating that the high degree of order seen in the allyl region of the X-ray structures is a consequence of crystallization.

The fact that allyl group mobility in solution differs from that observed in the crystal may be important in light of several recent findings. FK506 and rapamycin exhibit nearly identical contacts with FKBP-12 in the so-called binding region (which includes the pipecolinyl and pyranose rings), with the protein backbone differing only slightly between the two complexes [11,12]. However, the FK506/FKBP-12 complex inhibits the Ca^{2+}-dependent phosphatase activity of calcineurin, while the rapamycin/FKBP-12 and 506BD/FKBP-12 complexes do not [6]. Together, these findings suggest that the solvent exposed edge of FK506 (which includes the allyl group) in the FK506/FKBP-12 complex could be part of a recognition site for the formation of a higher order complex with calcineurin. Drug design strategies based upon the crystal structure must therefore allow for packing-induced distortions of the crucial allyl region.

Finally, our results indicate that caution is necessary when determining the conformation of bound ligands by restrained molecular dynamics. The conformation of a bound ligand is influenced by protein contacts and can obviously differ greatly from the lowest energy conformation of the unbound form. When restrained molecular dynamics refinement is performed on a bound ligand in the absence of the receptor, the danger exists that regions of the ligand that are poorly restrained by NOEs will adopt conformations that are influenced by the force field of the free ligand. Refinement methods that beter represent the limitations of the NOE restraints, such as MD using time-averaged restraints [32,33], are a useful means to avoid overestimating the precision of the final structures.

Acknowledgements: ^{13}C-FK506 was produced and supplied by Chugai Pharmaceutical Co., Ltd, using a germline kindly provided by K. Nagai at Tokyo Institute of Technology. We are indebted to S. Chambers for overexpressing hrFKBP-12, and M. Fitzgibbon and J. Black for assisting with the purification; D. Pearlman for performing time-averaged restraint calculations and critical reading of the manuscript. We wish to thank M. Rance, A. Palmer, and W. Fairbrother (Research Institute of Scripps Clinic), and M. Yamashita for helpful discussions.

REFERENCES

[1] Schreiber, S.L. (1991) Science 251, 283–287.
[2] Tocci, M.J., Matkovich, D.A., Collier, K.A., Kwok, P., Dumont, F., Lin, S., Degudicibus, S., Siekierka, J.J., Chin, J. and Hutchinson, N.I. (1989) J. Immunol. 143, 718–726.
[3] Mattila, P.S., Ullman, K.S., Fiering, S., Emmel, E.A., McCutcheon, M., Crabtree, G.R. and Herzenberg, L.A. (1990) EMBO J. 9, 4425–4433.
[4] Flanagan, W.M., Corthesy, B., Bram, R.J. and Crabtree, G.R. (1991) Nature 352, 803–807.
[5] Bierer, B.E., Mattila, P.S., Standaert, R.F., Herzenberg, L.A., Burakoff, S.J., Crabtree, G. and Schreiber, S.L. (1990) Proc. Natl. Acad. Sci., USA 87, 9231–9235.
[6] Liu, J., Farmer, J.D., Lane, W.S., Friedman, J., Weissman, I. and Schreiber, S.L. (1991) Cell 66, 807–815.
[7] Moore, J.M., Peattie, D.A., Fitzgibbon, M.J. and Thomson, J.A. (1991) Nature 351, 248–250.
[8] Michnick, S.W., Rosen, M.K., Wandless, T.J., Karplus, M. and Schreiber, S.L. (1991) Science 252, 836–839.
[9] Ke, H., Zydowsky, L.D., Liu, J. and Walsh, C.T. (1991) Proc. Natl. Acad. Sci. USA 88, 9483–9487.
[10] Kallen, J., Spitzfaden, C., Zurini, M.G.M., Wider, G., Widmer, H., Wüthrich, K. and Wilkinshaw, M.D. (1991) Nature 353, 276–279.
[11] Van Duyne, G.D., Standaert, R.F., Karplus, P.A., Schreiber, S.L. and Clardy, J. (1991) Science 252, 839–842.
[12] Van Duyne, G.D., Standaert, R.F., Schreiber, S.L. and Clardy, J. (1991) J. Am. Chem. Soc. 113, 7433–7434.
[13] Fesik, S.W., Gampe, R.T., Eaton, H.L., Gemmecker, G., Olejniczak, E., Neri, P., Holzman, T.F., Egan, D.A., Edalji, R., Simmer, R., Helfrich, R., Hochlowski, J. and Jackson, M. (1991) Biochemistry 30, 6574–6583.

[14] Weber, C., Wider, G., von Freyberg, B., Traber, R., Braun, W., Widmer, H. and Wüthrich, K. (1991) Biochemistry 30, 6563–6574.
[15] Petros, A.M., Gampe, R.T., Gemmecker, G., Neri, P., Holzman, T.F., Edalji, R., Hochlowski, J., Jackson, M., McAlpine, J., Luly, J.R., Pilot-Matias, T., Pratt, S. and Fesik, S.W. (1991) J. Med. Chem. 34, 2928–2931.
[16] Yamashita, M. and Navia, M., in preparation.
[17] Kino, T., Hatanaka, H., Hashimoto, M., Nishiyama, M., Goto, T., Kohsaka, M., Aoki, H. and Imanaka, H. (1987) J. Antibiotics 40, 1249–1255.
[18] Tsuji, R.F., Yamamoto, M., Nakamura, A., Kataoka, T., Magae, J., Nagai, K. and Yamasaki, M. (1990) J. Antibiotics 10, 1293–1301.
[19] Eccles, C., Billeter, M., Güntert, P. and Wüthrich, K., (1989) Abstracts of the Xth Meeting of the International Society for Magnetic Resonance.
[20] Norwood, T.J., Boyd, J., Heritage, J.E., Soffe, N. and Campbell, I. (1990) J. Magn. Reson. 87, 488.
[21] Bax, A., Ikura, M., Kay, L.E., Torchia, D. and Tshudin, R. (1990) J. Magn. Reson. 86, 304.
[22] Otting, G. and Wüthrich, K. (1989) J. Magn. Reson. 85, 586.
[23] Otting, G. and Wüthrich, K. (1990) Quat. Rev. Biophys. 23, 39.
[24] Rance, M., Sorenson, O.W., Bodenhausen, G., Wagner, G., Ernst, R.R. and Wüthrich, K. (1983) Biochem. Biophys. Res. Commun., 117, 469.
[25] Bodenhausen, G., Kogler, H. and Ernst, R.R. (1984) J. Magn. Res., 58, 370.
[26] Cavanagh, J. and Rance, M. (1990) J. Magn. Reson. 88, 72.
[27] Braunschweiler, L., Bodenhausen, G. and Ernst, R.R. (1984) Mol. Phys. 48, 535.
[28] Rance, M. and Wright, P.E. (1986) J. Magn. Reson. 66, 372.
[29] Havel, T.F. (1991) Prog. Biophys. Mol. Biol. 56, 43–78.
[30] Easthope, P. and Havel, T.F. (1988) Discrete Applied Math. 19, 129.
[31] Wandless, T.J., Michnick, S.W., Rosen, M.K., Karplus, M., Schreiber, S. (1991) J. Am. Chem. Soc. 113, 2339.
[32] Torda, A.E., Scheek, R.M. and van Gunsteren, W.F. (1989) Chem. Phys. Lett. 157, 289–294.
[33] Pearlman, D.A. and Kollman, P.A. (1991) J. Mol. Biol. 220, 457–479.
[34] Petros, A.M., Neri, P. and Fesik, S.W. (1992) J. Biomol. NMR 2, 11–18.
[35] Karuso, P., Kessler, H. and Mierke, D.F. (1990) J. Am. Chem. Soc. 112, 9434–9436.
[36] Mierke, D.F., Schmieder, P., Karuso, P. and Kessler, H. (1991) Helv. Chim. Acta 74, 1027–1047.
[37] Shaka, A.J., Keeler, J. and Freeman, R.R. (1983) J. Magn. Reson. 53, 313–340.
[38] Shaka, A.J., Barker, P.B. and Freeman, R.R. (1985) J. Magn. Reson. 64, 547.